Chirality dependence of the density-of-states singularities in carbon nanotubes

S. Reich and C. Thomsen
Institut für Festkörperphysik, Technische Universität Berlin, Hardenbergstrasse 36, 10623 Berlin, Germany
(Received 22 February 2000)

We derive an approximate analytical expression for the density-of-states singularities in single-walled carbon nanotubes. Our approximation goes beyond the lowest-order, isotropic approach and yields the energy splitting for an arbitary chiral angle in metallic nanotubes. Semiconducting tubes are shown to fall into two classes and have a corresponding energy shift, which should be observable experimentally.

The unique one-dimensional structure of carbon nanotubes and the related electronic band structure have been of much interest. Hamada *et al.* noticed in their calculation that there was a difference in electronic structure of armchair and zigzag nanotubes, the two limiting chiral angles.[1] In plots of energy versus diameter by Mintmire *et al.* and later Kataura *et al.* it became evident that similar diameters but different chiral angles produced slight differences in energies of the singularity.[2,3] Smaller diameters enhanced this dispersion. White and Mintimire showed that to first approximation the energy of the singularity is independent of chirality and should not depend on the size of the unit cell.[4–6] In a further analysis in this approximation the density of states of nanotubes was expressed as a universal function that does not depend on chirality.[7] The first-order expression for the energy is widely used as a basis for the analysis of experimental work on the singularities.[8–11]

Recently, it was pointed out that deviations from a circle in the energy contours near the Fermi surface produce a splitting of the singularity in metallic tubes (trigonal warping effect),[7,12,13] which is maximal for zigzag tubes. Saito *et al.* give an analytical expression for this limiting case.[13] Their plot of the density of states of selected nanotubes with similar diameters and different chiral angles α suggests that the splitting decreases continuously as α is varied from $\alpha=0°$ (zigzag topology) to 30° (armchair), and it is zero for the armchair configuration.

In this paper we generalize these results to arbitrary chiral angles and derive an approximate analytical expression for the energy splitting of the density-of-states singularities of metallic carbon nanotubes and find the related shift for semiconducting nanotubes. The starting point of our analysis is the tight-binding expression for the energy of a graphene sheet:

$$\varepsilon(\tilde{\mathbf{k}}) = \pm\,\gamma_0\{3 + 2\cos\tilde{\mathbf{k}}\cdot\mathbf{R}_1 + 2\cos\tilde{\mathbf{k}}\cdot\mathbf{R}_2 + 2\cos\tilde{\mathbf{k}}\cdot(\mathbf{R}_1-\mathbf{R}_2)\}^{1/2}, \tag{1}$$

where $\mathbf{R}_1$ and $\mathbf{R}_2$ denote the unit-cell vectors of the graphene sheet. This approach to the electronic structure of carbon nanotubes implies that a nanotube can be looked at as a wrapped-up graphite sheet. Curvature effects on the electronic and vibrational energies are on the order of 10^{-2}, as shown by ab initio calculations[14] and second-order Raman spectra;[15] they will not be considered here.

The energy in the band structure of graphite goes to zero at the K point of the Brillouin zone. For the further analysis we transform Eq. (1) to one where $\mathbf{k}=\tilde{\mathbf{k}}-\mathbf{k}_\mathbf{F}$ represents a vector originating in the K point:

$$E(\mathbf{k}) = \pm\,\gamma_0\{3 - \cos\mathbf{k}\cdot\mathbf{R}_1 - \cos\mathbf{k}\cdot\mathbf{R}_2 - \cos\mathbf{k}\cdot(\mathbf{R}_1-\mathbf{R}_2) + \sqrt{3}\sin\mathbf{k}\cdot\mathbf{R}_1 - \sqrt{3}\sin\mathbf{k}\cdot\mathbf{R}_2 - \sqrt{3}\sin\mathbf{k}\cdot(\mathbf{R}_1-\mathbf{R}_2)\}^{1/2}. \tag{2}$$

In Fig. 1(a) we show energy contours of the expression (2)

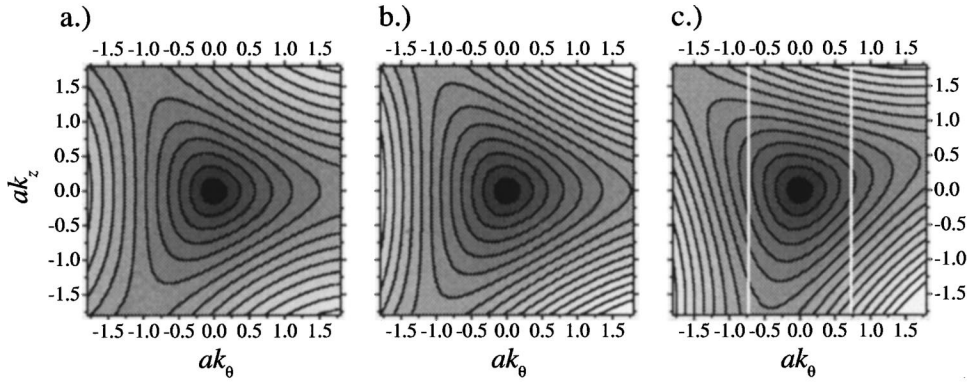

FIG. 1. (a) Energy contours near the K point of graphite according to the exact tight-binding expression of Eq. (2). The axes point in the circumferential (θ) and axial (z) directions of a zigzag nanotube ($\alpha=0°$). The length of the graphite unit cell vector is denoted by a. (b) Same as in (a) but in the approximation of Eq. (4). (c) Same as in (b) but for a chiral angle of $\alpha=15°$. The vertical lines touch tangentially the energy contours in the density-of-states singularities.

near the K point of the Brillouin zone, i.e., around zero in $\mathbf{k}$. It is nicely seen how, for increasing $|\mathbf{k}|$, the energy contours change from a circular to a more triangular shape.

In carbon nanotubes the wave vector $\mathbf{k}=(k_\theta,k_z)$ is quantized in k_θ, while k_z can take continuous values. The singularities in the density of states (DOS) near the Fermi level, according to Mintmire and White,[7] are given by the zeros in the derivative of the energy with respect to the wave vector component k_z. In the type of plot in Fig. 1 this corresponds to tangentials to the energy contours running parallel to the k_z axis. The other k component k_θ is given by the boundary condition in the circumferential direction:

$$k_\theta=\mathbf{k}\cdot\mathbf{R}=\frac{2\pi}{3|\mathbf{R}|}(3m-n_1+n_2)=\frac{2}{3d}(3m-n_1+n_2), \tag{3}$$

where $\mathbf{R}=n_1\mathbf{R}_1+n_2\mathbf{R}_2$ is the chiral vector along which the tube is wrapped up, m is an integer, and n_1 and n_2 are the commonly used indices to describe the chirality of the tube. The diameter and chiral angle are given in terms of these indices and the graphite lattice constant a by

$$d=\frac{a}{\pi}\sqrt{n_1^2+n_2^2+n_1n_2} \quad \text{and} \quad \tan(30°-\alpha)=\frac{1}{\sqrt{3}}\frac{n_1-n_2}{n_1+n_2}.$$

In order to obtain an analytical expression for the energy of the singularities, we expand Eq. (2) to third order (under the square root) in $\mathbf{k}$ and find

$$E(a\mathbf{k})\approx\pm\gamma_0\left\{\frac{3}{4}(ak)^2-\frac{\sqrt{3}a^3}{8}[k_\theta(k_\theta^2-3k_z^2)\cos 3\alpha - k_z(k_z^2-3k_\theta^2)\sin 3\alpha]\right\}^{1/2}, \tag{4}$$

where $k=|\mathbf{k}|$. Note that the angular functions vary with 3 times the chiral angle, introducing the triangular shape in the energy contours around the K point. The fourth-order term $(-3/64)(ak)^4$, like the k^2 term, depends on the magnitude of $\mathbf{k}$ and does not enhance the deviation from circular symmetry; its contribution to the energy is small for not too large ak_θ, and we will discuss it later. In Fig. 1(b) we show the contours calculated in the approximation given by Eq. (4) on the same scale as in Fig. 1(a); they describe very well the energies in the vicinity of the K point. For other chiral angles the triangle rotates by α around its center at $k=0$. As an example of a chiral tube we show the Brillouin zone near K corresponding to a (14, 5) tube ($\alpha=15°$) in Fig. 1(c). In the limit of an armchair nanotube ($\alpha=30°$) the tip of the triangle points in the $(-k_z)$ direction.

The two vertical lines in Fig. 1(c) at $ak_\theta^{\pm}=\pm 0.74$, which, according to Eq. (3) define the energy of the second singularity for the metallic (14, 5) nanotube, are seen to touch different energy contours. For $ak_\theta^{-}=-0.74$ the line is tangential slightly above the fourth contour whereas the other line is tangential somewhat below the fourth contour, at a smaller k_z value. The difference in these two energies corresponds to the energy splitting of the singularities for this particular chiral angle. It is obvious from Fig. 1 for symmetry reasons that a metallic zigzag tube has the maximum energy splitting (for a given diameter) and that an armchair tube has no splitting at all.

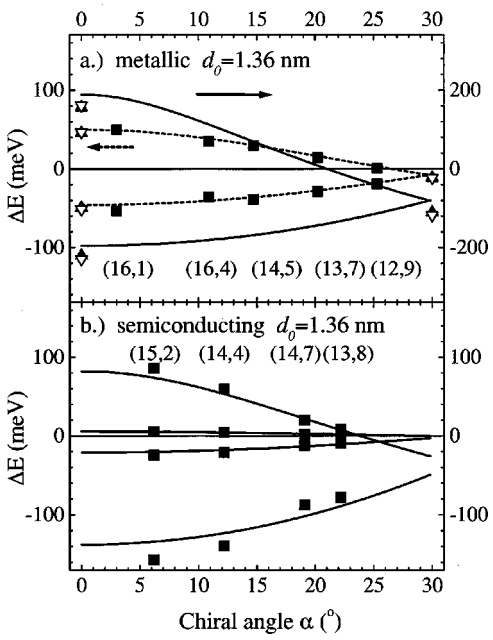

FIG. 2. (a) Energy splitting of the DOS singularity in metallic nanotubes as function of chiral angle; the energy calculated according to Eq. (7) was taken as reference. The solid curve (right axis) corresponds to the second singularity, e.g., of a (10, 10) nanotube, the dashed curve (left axis) to the first one. Upper and lower branches belong to k_θ^- and k_θ^+, respectively. The fourth-order approximation (open triangles) and the exact solution (solid triangles) for the zigzag and armchair topologies are shown for comparison. The solid squares are values for selected metallic tubes as indicated. (b) Same as (a) but for semiconducting tubes. The curves are valid for the class of semiconducting tubes where $\mathrm{sgn}[\min(3m-n_1+n_2)]=-1$, as is the case for the selection of tubes shown.

We use the approximation of Eq. (4) to calculate for an arbitrary chiral angle the ak_z values of the singularity, i.e., the points at which $dE/d(ak_z)=0$:

$$ak_{z_{1,2}}=\frac{2}{\sqrt{3}\sin 3\alpha}\left(-1-\frac{\sqrt{3}}{2}ak_\theta\cos 3\alpha \pm\sqrt{1+\sqrt{3}ak_\theta\cos 3\alpha+\frac{3}{4}(ak_\theta)^2}\right). \tag{5}$$

Only the plus solution yields an ak_z value near the K point and will be considered further. The two values of $ak_\theta=\pm 0.74$, inserted into Eq. (6) give two values $k_z^{\pm}$. For the example of Fig. 1(c) this corresponds to $ak_z^-=0.26$ and $ak_z^+=0.11$. The energy splitting is now readily obtained from Eq. (4):

$$\delta E=E(ak_z^-)-E(ak_z^+). \tag{6}$$

For our above example we find $\delta E=1.91-1.67\,\mathrm{eV}=0.24\,\mathrm{eV}$, where we used $\gamma_0=2.9\,\mathrm{eV}$ as is consistent with Raman experiments.[10,11,16] This value of δE agrees with Saito *et al.*[13] and may be read off from their Fig. 4 for the (14, 5) tube. The metallic tubes thus have degenerate singu-

larities in the armchair topology (and in the isotropic approximation), which split for a general chiral angle according to Eq. (6).

As Eq. (4) is an analytical solution for arbitrary chiral angles, we may calculate the energy splitting as function of α. In Fig. 2(a) we have plotted the difference in energy, ΔE, between our and the first-order approximation versus α for the first and second singularities of metallic tubes with a diameter near $d_0 = 1.36\,\mathrm{nm}$ [corresponding to a (10, 10) tube]. Also shown are the shifts in energy, ΔE, for some selected tubes with diameters within ± 0.1 nm of the chosen d_0. The energies deviate slightly from the curves for a particular chirality because of different actual diameters. The splitting of the singularities δE is seen to decrease monotonically for increasing α, starting horizontally at $\alpha = 0°$ and going towards zero with a finite slope at $\alpha = 30°$. The splitting is nonlinear in ak_θ; larger ak_θ yield much larger splittings as evident from the figure, where we plotted ΔE on different scales. Neglecting the k^3 term in Eq. (4) and with $k \equiv k_\theta$ yields Mintmire and White's[7] result of

$$E = \frac{\sqrt{3}}{2}\gamma_0 ak, \tag{7}$$

the isotropic approximation of the energy in the *K*-point vicinity and the zeros of our plots in Fig. 2. Note that their result does not coincide with the value for armchair topology but lies above that. For larger ak_θ, i.e., smaller tubes or higher singularities, this deviation increases.

The plots of ΔE are remarkably asymmetric with respect to the armchair energy in contrast to what was reported by Ref. 13. For $ak_\theta = 0.36$ [dashed curve in Fig. 2(a)] the upper branch shifts by a factor of 1.3 more than the lower one: for $ak_\theta = 0.72$ (solid curve) it is 2.5 times as much (calculated from the fourth-order approximation at $\alpha = 0°$). This implies that if the resolution in an experiment is not large enough to resolve a splitting, there is nevertheless a shift of the singularities of metallic tubes from the armchair value associated with a broadening which should be observable.

The situation is different for semiconducting tubes. As can be seen in Eq. (3), k_θ varies in steps of $2/d$ when *m* steps through integers; the k_θ values are not symmetric around $k_\theta = 0$. There is no degeneracy in the isotropic approximation and hence there cannot be any splitting. There is, however, a shift from the limiting $\alpha = 30°$ energy value as well, as the same triangular shape as for metallic tubes is present. We show this for four different values of *m* in Fig. 2(b). A further complication arises because the smallest allowed k_θ for semiconducting tubes may be either negative or positive. In Fig. 2(b) we have indicated explicitly tubes that have $\mathrm{sgn}[\min(3m - n_1 + n_2)] = -1$. The four points shown for each selected tube correspond to subsequent singularities starting from the lowest one, which shows the smallest $|\Delta E|$. The largest singularity shown for the (15, 2) tube has an absolute energy of 1.39 eV and is shifted by 130 meV compared to what is calculated from Eq. (7). For the other type semiconducting tubes, e.g., (15, 4), the dependence of ΔE on α is different since Eq. (4) is not symmetric with respect to the sign of k_θ. Experimentally, with a limited resolution, the shift in semiconducting tubes may be easier to observe since a shift is more readily detected than a broadening or splitting.

Finally, we discuss some limiting cases of our solution and the accuracy of the approximations. In the armchair tubes ($\alpha = 30°$) our expression for k_z in Eq. (5) reduces to $ak_z = -2/\sqrt{3} + \sqrt{4/3 + (ak_\theta)^2}$ and an energy of

$$E^{\pm}_{k_z} = \gamma_0 \left[\frac{3}{4}(ak)^2 + \frac{\sqrt{3}}{8} a^3 k_z (k_z^2 - k_\theta^2) \right]^{1/2} \quad \text{(armchair tubes)}.$$

Since k_θ appears only in even order, $\delta E^{\mathrm{AC}} = 0$. In the zigzag case $k_z^{\pm} = 0$; i.e., the splitting in metallic tubes is maximal where the tangentials meet the ak_θ axis. The energies in these points are

$$E^{\pm}_{k_z} = \frac{\sqrt{3}}{2}\gamma_0 |ak_\theta| \times \left[1 \mp \frac{1}{2\sqrt{3}} ak_\theta \right]^{1/2} \quad \text{(metallic zigzag tubes)}.$$

Here the energy splitting (6) is

$$\delta E^{\mathrm{ZZ}} = \frac{\sqrt{3}}{2}\gamma_0 |ak_\theta| [\sqrt{1 + ak_\theta/2\sqrt{3}} - \sqrt{1 - ak_\theta/2\sqrt{3}}] \approx \gamma_0 (ak_\theta)^2/4.$$

For $ak_\theta = 0.73$ this corresponds to 0.38 eV, which is equal to the maximal splitting in metallic tubes with $d = 1.4$ nm observed in Fig. 4 of Ref. 13.[17] In Fig. 2(a) we show on the same scale the values of ΔE as derived numerically from the exact expression (2) and including the fourth-order term in our approximation (4). It is seen that the curves (correct to third order in *k*) yield close results; the fourth order cannot be distinguished from the exact value for the ak_θ value shown. Our approximation should be good at least to $|ak_\theta| = 1$, where the errors for all absolute energies are less than 4% (third order) and less than 0.7% (fourth order).

In conclusion, we derived an approximate analytical solution to the energies of the singularities in the density of states of metallic and semiconducting carbon nanotubes with arbitrary indices (n_1, n_2) for energies not too far from the Fermi surface ($|ak| \leqslant 1$). The energies of the singularities in the density of states in carbon nanotubes shift due to the trigonal distortion of the energy contours near the *K* point. Metallic tubes, which are doubly degenerate in the isotropic approximation, split for a general chiral angle. Semiconducting nanotubes are nondegenerate in the isotropic approximation, so they cannot split; their absolute energies shift, though, as a function of α, by an amount given by the same expression as for metallic tubes with the appropriate k_θ values. Semiconducting chiral tubes fall into two classes, depending on the sign of their smallest allowed k_θ values. Experimentally their shift may be easier to observe than the lifting of the degeneracy of metallic tubes. Our results should be useful when finding splittings or shifts in the DOS singularities of specific nanotubes, with an arbitrary but known chirality or in ensembles of tubes with a known, possibly nonuniform chirality distribution.

[1] N. Hamada, S. Sawada, and A. Oshiyama, Phys. Rev. Lett. **68**, 1579 (1992).
[2] J. W. Mintmire, D. H. Robertson, and C. T. White, J. Phys. Chem. Solids **54**, 1835 (1993).
[3] H. Kataura, Y. Kumazawa, Y. Maniwa, I. Umezu, S. Suzuki, Y. Ohtsuka, and Y. Achiba, Synth. Met. **103**, 2555 (1999).
[4] C. T. White and J. W. Mintmire, Nature (London) **394**, 29 (1998).
[5] M. S. Dresselhaus, Nature (London) **391**, 19 (1998).
[6] J. C. Charlier and P. Lambin, Phys. Rev. B **57**, 15 037 (1998).
[7] J. W. Mintmire and C. T. White, Phys. Rev. Lett. **81**, 2506 (1998).
[8] T. W. Odom, J. L. Huang, P. K. M. Ouyang, and C. M. Lieber, J. Mater. Res. **13**, 2380 (1998).
[9] J. W. G. Wildöer, L. C. Venema, A. G. Rinzler, R. E. Smalley, and C. Dekker, Nature (London) **391**, 59 (1998).
[10] M. A. Pimenta, A. Marucci, S. A. Empedocles, M. G. Bawendi, E. B. Hanlon, A. M. Rao, P. C. Eklund, R. E. Smalley, G. Dresselhaus, and M. S. Dresselhaus, Phys. Rev. B **58**, 16 016 (1998).
[11] P. M. Rafailov, H. Jantoljak, and C. Thomsen, Phys. Rev. B (to be published).
[12] P. Kim, T. W. Odom, J.-L. Huang, and C. M. Lieber, Phys. Rev. Lett. **82**, 1225 (1999).
[13] R. Saito, G. Dresselhaus, and M. S. Dresselhaus, Phys. Rev. B **61**, 2981 (2000).
[14] D. Sánchez-Portal, E. Artacho, J. Soler, A. Rubio, and P. Ordejón, Phys. Rev. B **59**, 12 678 (1999).
[15] C. Thomsen, Phys. Rev. B **61**, 4542 (2000).
[16] M. Milnera, J. Kürti, M. Hulman, and H. Kuzmany, Phys. Rev. Lett. **84**, 1324 (2000).
[17] Expression (19) of Ref. 13 (not the corresponding peaks in their Fig. 4) contains an additional factor of 2 which does not follow from their Eqs. (7) and (18).